

Distributed Reflector Structure and Diffraction Grating Structure in the Solar Cell

Roghaye Ghorbanpour¹, Navid Taghizadegan²

¹Department of Electrical Engineering, Ahar Branch, Islamic Azad University, Ahar, Iran
ru.ghourbanpor@yahoo.com

²The faculty of Electrical Engineering of the University of Madani Azerbaijan
Ntaghizadegan@yahoo.com

Abstract

Today, due to qualitative growth and scientific advances, energy, especially electricity is increasingly needed by human society. One of the almost endless and pure energy which have been paid attention over the years is the solar energy. Solar cells directly convert solar energy into electrical energy and are one of the main blocks of photovoltaic systems. Significant improvement has been made in the performance of solar cells since their introduction. Improvement of parameters such as cell efficiency, solar spectrum absorption and manufacturing costs which are key parameters in the process of cell development. The crystalline type is commonly used to achieve a lower recombination and higher absorption coefficient, and other types of silicon that have high recombination and low absorption coefficient, leading to a sharp drop in cell efficiency are not used as much. Different kinds of light trapping techniques and effective photons trapping using some fibered structures and various types of reflecting structures and light scattering, etc., have been proposed. In this paper, distributed Bragg reflector structure and also diffraction grating structure are used. In both structures, determination of the optimum material and also geometric properties to achieve maximum improvement in efficiency have taken into consideration.

Keywords: Silicon solar cells, light trapping, distributed Bragg reflector, diffraction grating

1- Introduction

Today, the major human needs for energy are often provided by fossil fuels. Fossil sources other than coal, could have survived up to the next century. Therefore, limited fossil fuel resources and the high costs of their use and conversion have forced man to switch to renewable energies. However, solar radiation sends earth 900 billion MW/h

of energy annually. This amount is 10 thousand times greater than the energy requirements of the man across the globe, and is equivalent of 0.48 billion barrels of crude oil. Due to the weight of sun which is about 333 thousand times of the weight of the earth, this luminous star can be seen as the huge source of energy for 5 billion years. As a result, growth in global energy consumption in the last century with an

increase in greenhouse gas emissions, is associated with more polluted environment and irreparable damage to vital resources. In order to reduce global dependence on exhaustible natural resources and environment damaging fuels, many scientific efforts have been done to reduce the cost of energy production from renewable sources. Therefore, switching to new energy sources that are somewhat endless and do not make the air polluted is inevitable. About fifty years ago, research on the use of solar energy has entered a new phase and important practical and scientific experiments have been carried out in this field, and now they are being conducted more extensively. In this study, silicon cells with 1.1 eV forbidden band energy and 5.4 Å lattice constant are considered. When light is absorbed by a material, light photons give energy to electrons in order to move them to a higher level. In metallic materials, excited electrons return to their original energy level after a short time, but the situation is different in semiconductor materials. So the forbidden band energy of the semiconductor determines how to react to the incident light. By radiating light on the solar cell, electrons and holes are produced in solar cells. The energy needed to create an electron-hole pair is equal to the forbidden band energy (E_g) of the semiconductor. Since the absorption coefficient of silicon in the range of visible light, where maximum of solar radiation is there too, is low, some of photons that entered the cell body are not absorbed. Although there are some different categories of solar cells, generally they can be categorized in many classes including

crystalline silicon solar cells, thin-film technology, multi-junction cells of group III-V, dye-sensitized Solar Cell (DSSC), polymer cells, and solar cells with quantum structures such as quantum wells and dots [2]. Today's market of solar cells belongs to silicon which is also considered the oldest and most widely-used semiconductor. Now more than 95% of solar photovoltaic components worldwide are made based on thin crystalline silicon tablets [3].

The highest technologic concentration in photovoltaic industry is on silicon. Crystalline silicon solar cells will be available for years to come due to the vast resources of silicon in the Earth's crust. Conversion efficiency has been obtained about 25% in research laboratories, but it is 23% in made cells [4]. Other reasons for the increasing growth of silicon cells include nontoxicity and low-waste manufacturing cycle. Solar cells that use hydrogenated amorphous silicon (a-Si:H) are absorbent, because it has a very high absorption coefficient [5]. However, despite the encouraging results of the a-Si:H [6], factors such as low absorption coefficient at long wavelengths and bulk recombination lead to study of other types to replace this material for use in solar cells with less thickness. Today, in particular, crystalline silicon (c-Si), amorphous-silicon (a-Si), and polycrystalline silicon (poly-Si) are used. Of all possible types, using crystalline silicon layers which are able to dramatically reduce the bulk recombination is very popular compared to amorphous and polycrystalline silicon layers. In other words, a number of photons will not be absorbed in the solar cell

but passes the cell's silicon layer and hit the metal fittings, thus their energy is wasted as heat. The heat increases the overall resistance of the cell and adversely affects its overall efficiency. However, the energy conversion efficiency of thin film cells is much less than thicker cells. This is due to reduced optical path length that limits the absorption efficiency and enhances the recombination process of carriers. For example, in ultra-thin film solar cells, the absorption in red and infrared wavelengths is not suitable enough to create good conversion efficiency [7].

Therefore, controlling the light entered into the cell and the absorption of this light in the range of long wavelengths is of prime importance, and this is the purpose of light trapping. In other words, in today's cells we face a serious problem called "no absorption of photons" which is mainly due to the reduction of cell space or simply reduction of optical path length for photons, and this is one of the most important reasons for the reduction in cell energy conversion efficiency in thinner cells compared to thicker ones. In recent years, many efforts have been done to increase the absorption of photons in the solar cell. Given the maturity that has been created today in the field of nano-photonics, different trapping techniques including optical crystals, diffraction gratings, anti-reflective coatings and metallic nano-structures like plasmonic are used [8]. In this research, photonic structures such as distributed Bragg reflector (DBR) and diffraction grating have been investigated. These structures have been used to reflect light into the active and

silicon region of cells which increases the cell's internal quantum efficiency and ultimately increases the overall efficiency of the cell. In order to make the issue of solar cells applicable, cells available in the market are used to provide street lights, and the feasibility of the project has been discussed. Then, using necessary simulations, strengths and weaknesses of the project are evaluated.

In this study, the arrangement of the chapters is so that in the second, the structures used in the study including Bragg reflector and diffraction grating are mentioned in detail. Mathematical relations of these structures are provided, their role in increasing the solar cell efficiency is investigated. In the third chapter, made designs for the back structures of cells are given and simulation results are also presented. In this section, R soft software package is used for simulation. Paper comes to an end with results explanation and summing up the measures taken.

2- Analysis of distributed Bragg reflector (DBR) and diffraction grating structures

It is explored for calculation of the diffusion matrix and adaption of the uniform and plane waves that are emitted perpendicular to the surface. Using the boundary conditions for these waves, progressive and regressive waves which are located at one side of the interface border are linked to waves in other side, and their relations are expressed in the form of a matching matrix. If there are several interface borders, progressive and regressive

waves are transmitted from an interface borderline to one using a 2x2 diffusion matrix. Different environments having different borders can be analyzed by a combination of matching and diffusion matrixes and the results can be presented in the form of a transfer (or transition) matrix.

2-1-Diffusion Matrix

In this section, we will first talk about the diffusion matrix. First, we consider a field which is polarized in x direction and is transmitted in z direction, in a lossless dielectric (homogeneous and isotropic) environment. Then we consider [9]:

$$E(z) = \hat{x}E_x(z) = \hat{x}E(z) \quad (1)$$

$$H(z) = \hat{y}H_y(z) = \hat{y}H(z) \quad (2)$$

Then we have:

$$E(z) = E_{0+}e^{-jkz} + E_{0-}e^{jkz} = E_+(z) + E_-(z) \quad (3)$$

$$H(z) = \frac{1}{\eta}(E_{0+}e^{-jkz} - E_{0-}e^{jkz}) = \frac{1}{\eta}(E_+(z) - E_-(z)) \quad (4)$$

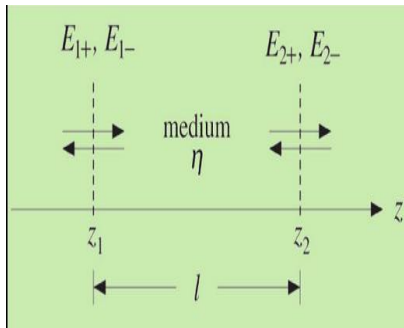


Fig.1.Transmission of a field between two points in a material space

where $\eta = \sqrt{\frac{\mu}{\epsilon}}$ is the environment characteristic impedance. To calculate the diffusion matrix, first we consider an environment according to Figure (1) where the electric and magnetic waves would spread in. The distance between the two points, from z_1 to z_2 is considered as $l = z_2 - z_1$. Progressive fields for places of z_1 to z_2 are determines as follows:

$$E_{2+} = E_{0+}e^{-jkz_2} \quad (5)$$

$$E_{1+} = E_{0+}e^{-jkz_1} = E_{0+}e^{-jk(z_2-l)} = e^{jkl}E_{2+} \quad (6)$$

It can be easily proved that for the progressive fields we have:

$$E_{1-} = e^{-jkl}E_{2-} \quad (7)$$

Thus, for both progressive and regressive waves, the matrix can be written as follows:

$$\begin{bmatrix} E_{1+} \\ E_{1-} \end{bmatrix} = \begin{bmatrix} e^{jkl} & 0 \\ 0 & e^{-jkl} \end{bmatrix} \begin{bmatrix} E_{2+} \\ E_{2-} \end{bmatrix} \quad (8)$$

The above matrix is called the diffusion matrix for progressive and regressive waves. Surge impedance transmission is as follows (assuming that $l = \frac{\lambda}{4}$):

$$Z_1 = \frac{\eta^2}{Z_2} \quad (9)$$

2-2-Matching matrix

In this section, we will examine the matching conditions at the borders. We consider a blade that has a border between two dielectric environments which has impedance characteristics of η and η' . Figure 2 shows this clearly:

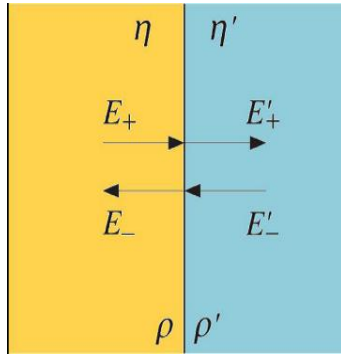


Fig.2. Interface border between dielectric and conductive environments [10].

The case of boundary conditions requires that the total electric and magnetic field be continuous on the two sides of the interface border. In other words, electromagnetic field continues across the dielectric environment. Therefore, we have [10]:

$$E = E' \quad (10)$$

$$H = H' \quad (11)$$

According to the definitions of progressive and regressive fields, we have:

$$E_+ + E_- = E'_+ + E'_- \quad (12)$$

$$\frac{1}{\eta}(E_+ - E_-) = \frac{1}{\eta'}(E'_+ - E'_-) \quad (13)$$

In the two equations above, if we obtain E_{\pm} in terms of E'_{\pm} , then we reach the following matrix equation:

$$\begin{bmatrix} E_+ \\ E_- \end{bmatrix} = \frac{1}{\tau} \begin{bmatrix} 1 & \rho \\ \rho & 1 \end{bmatrix} \begin{bmatrix} E'_+ \\ E'_- \end{bmatrix} \quad (14)$$

If we arrange E'_{\pm} in terms of E_{\pm} , we obtain the following equation:

$$\begin{bmatrix} E'_+ \\ E'_- \end{bmatrix} = \frac{1}{\tau'} \begin{bmatrix} 1 & \rho' \\ \rho' & 1 \end{bmatrix} \begin{bmatrix} E_+ \\ E_- \end{bmatrix} \quad (15)$$

The equations (14) and (15) are called matching matrix at the interface border between two environments. $\{\tau, \rho\}$ and $\{\tau', \rho'\}$ are respectively primary reflection and primary transfer in the first and second environments, and can be calculated by the following relations.

$$\rho = \frac{\eta' - \eta}{\eta' + \eta}, \tau = \frac{2\eta'}{\eta' + \eta} \quad (16)$$

$$\rho' = \frac{\eta - \eta'}{\eta + \eta'}, \tau' = \frac{2\eta}{\eta + \eta'} \quad (17)$$

impedance of both environments in the forms of $\eta = \frac{\eta_0}{n}$ and $\eta' = \frac{\eta_0}{n'}$ where η_0 is the characteristic impedance of vacuum environment which is equal to $\eta_0 = \sqrt{\frac{\mu_0}{\epsilon_0}}$, and

n and n' are the refractive index of two environments. According to the relations, (16) and (17) can be rewritten as follows:

$$\rho = \frac{n - n'}{n + n'}, \tau = \frac{2n}{n + n'} \quad (18)$$

$$\rho' = \frac{n' - n}{n' + n}, \tau' = \frac{2n'}{n' + n} \quad (19)$$

2-3-Analysis of the wave in a dielectric blade

Problems that have multiple environments can be analyzed by diffusion and matching matrixes. For example, Figure 3 shows a problem with two environments which is composed by a η_1 dielectric blade that separates two semi-infinite environments of η_a and η_b .

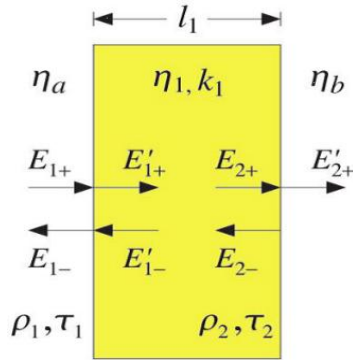


Fig.3.A dielectric blade

Where l_1 is the blade thickness, $k_1 = \frac{\omega}{c_1}$ wave number and $\lambda_1 = \frac{2\pi}{k_1}$ the wavelength within the dielectric. We also have $\lambda_1 = \frac{\lambda_0}{n_1}$, where λ_0 and n_1 are free space wavelength and dielectric refractive index, respectively. We assume that the field enters dielectric from η_a environment and η_b environment has only progressive wave. First, we calculate the amounts of primary reflection and primary transfer, and we have:

$$\rho_1 = \frac{n_a - n_1}{n_a + n_1}, \quad \tau_1 = 1 + \rho_1 \quad (20)$$

$$\rho_2 = \frac{n_1 - n_b}{n_1 + n_b}, \quad \tau_2 = 1 + \rho_2 \quad (21)$$

For analysis, we start from the left environment η_a and write the diffusion and matching matrixes respectively to reach the η_b environment. Thus, we have the following relations:

$$\begin{aligned} \begin{bmatrix} E_{1+} \\ E_{1-} \end{bmatrix} &= \frac{1}{\tau_1} \begin{bmatrix} 1 & \rho_1 \\ \rho_1 & 1 \end{bmatrix} \begin{bmatrix} E'_{1+} \\ E'_{1-} \end{bmatrix} = \frac{1}{\tau_1} \begin{bmatrix} 1 & \rho_1 \\ \rho_1 & 1 \end{bmatrix} \begin{bmatrix} e^{jk_1 l_1} & 0 \\ 0 & e^{-jk_1 l_1} \end{bmatrix} \begin{bmatrix} E_2 \\ E_2 \end{bmatrix} \\ &= \frac{1}{\tau_1} \begin{bmatrix} 1 & \rho_1 \\ \rho_1 & 1 \end{bmatrix} \begin{bmatrix} e^{jk_1 l_1} & 0 \\ 0 & e^{-jk_1 l_1} \end{bmatrix} \frac{1}{\tau_2} \begin{bmatrix} 1 & \rho_2 \\ \rho_2 & 1 \end{bmatrix} \begin{bmatrix} E'_{2+} \\ 0 \end{bmatrix} \end{aligned} \quad (22)$$

In (22) it is assumed that $E'_{2-} = 0$ because η_b environment is extremely uniform and has no change to reflect the wave. By multiplying the matrixes by the following values we will have:

$$E_{1+} = \frac{e^{jk_1 l_1}}{\tau_1 \tau_2} (1 + \rho_1 \rho_2 e^{-2jk_1 l_1}) E'_{2+} \quad (23)$$

$$E_{1-} = \frac{e^{jk_1 l_1}}{\tau_1 \tau_2} (\rho_1 + \rho_2 e^{-2jk_1 l_1}) E'_{2+} \quad (24)$$

Dielectric blade has reflection coefficient of R_1 to the wave passage, which is defined as follows:

$$\Gamma_1 = \frac{E_{1-}}{E_{1+}} = \frac{\rho_1 + \rho_2 e^{-2jk_1 l_1}}{1 + \rho_1 \rho_2 e^{-2jk_1 l_1}} \quad (25)$$

Is we assume $z^{-1} = e^{-2jk_1 l_1}$, then (25) can be rewritten as:

$$\Gamma_1(z) = \frac{E_{1-}}{E_{1+}} = \frac{\rho_1 + \rho_2 z^{-1}}{1 + \rho_1 \rho_2 z^{-1}} \quad (26)$$

2-4-Analysis of a quarter-wavelength thickness for dielectric blade

We use the zeros of the conversion function of equation (26) to analyze the dielectric blade thickness. According to these zeros, we can consider two scenarios: half-wavelength thickness and quarter-wavelength thickness. Obviously, conversion function zero is:

$$z = e^{2jk_1 l_1} = -\frac{\rho_2}{\rho_1} \quad (27)$$

Since in (27), the right side of the equation is real ($-\frac{\rho_2}{\rho_1}$) and the left side is dummy and has the same size too, conditions are so that only the two following amounts can be considered:

Half-wavelength thickness

$$l_1 = m \frac{\lambda_1}{2} \quad (28)$$

Quarter-wavelength thickness

$$l_1 = (2m+1) \frac{\lambda_1}{4} \quad (29)$$

Realization of equation (28) requires that $2k_1 l_1$ be an integer multiple of 2π and equal to $2k_1 l_1 = 2m\pi$, where m is an integer. The thickness of this mode is $l_1 = m \frac{\lambda_1}{2}$ where

λ_1 the wavelength in environment 1 is. Realization of equation (29) requires that $2k_1 l_1$ be an odd multiple of π and equal to $2k_1 l_1 = (2m+1)\pi$ where m is an integer.

In this mode, the thickness is $l_1 = (2m+1) \frac{\lambda_1}{4}$. Given the above relations,

reflection conversion function for both half- and quarter-wavelength can be rewritten as follows:

Half-wavelength thickness

$$\Gamma_1(z) = \frac{\rho_1(1-z^{-1})}{1-\rho_1^2 z^{-1}} \quad (30)$$

Quarter-wavelength thickness

$$\Gamma_1(z) = \frac{\rho_1(1-z^{-1})}{1+\rho_1^2 z^{-1}} \quad (31)$$

Where $z = e^{2jk_1 l_1} = e^{j\omega T}$ and ω is the wave angular frequency and T the time delay of

wave passage through environment 1. The relations are applicable for ω and T:

$$2k_1 l_1 = \omega \left(\frac{2l_1}{c_1} \right) = \omega T \quad (32)$$

$$T = \frac{2l_1}{c_1} = \frac{2n_1 l_1}{c_0} \quad (33)$$

We calculate the square size for reflection conversion function and after simplification we will achieve the following relationship:

Half-wavelength thickness

$$\begin{aligned} |\Gamma_1|^2 &= \\ &= \frac{2\rho_1^2 (1 - \cos(2k_1 l_1))}{1 - 2\rho_1^2 \cos(2k_1 l_1) + \rho_1^4} \\ &= \frac{2\rho_1^2 (1 - \cos(\omega T))}{1 - 2\rho_1^2 \cos(\omega T) + \rho_1^4} \end{aligned} \quad (34)$$

Quarter-wavelength thickness

$$\begin{aligned} |\Gamma_1|^2 &= \\ &= \frac{2\rho_1^2 (1 + \cos(2k_1 l_1))}{1 + 2\rho_1^2 \cos(2k_1 l_1) + \rho_1^4} \\ &= \frac{2\rho_1^2 (1 + \cos(\omega T))}{1 + 2\rho_1^2 \cos(\omega T) + \rho_1^4} \end{aligned} \quad (35)$$

If we draw equations (34) and (35) in terms of ω (the angular frequency of the wave), they will be in the form of Figure 4:

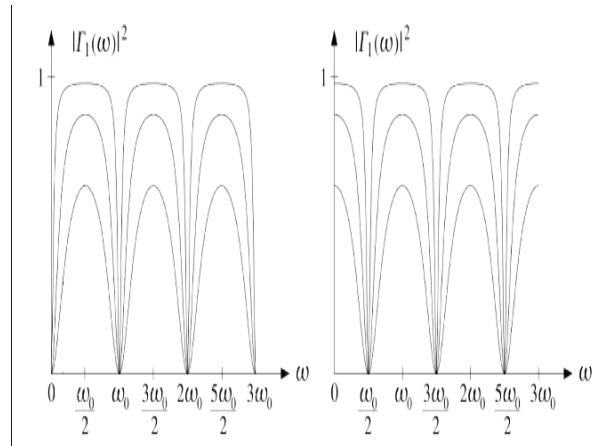


Fig.4. Normalized plot of reflection $|\Gamma_1|^2$

- Left: for half-wavelength thickness
- Right: for quarter-wavelength thickness.

As can be seen in Figure 4, in quarter-wavelength, the amount of reflection in the wavelength corresponding to the radiation wavelength - ω_0 - has the maximum value, but in the same case in half-wavelength, the amount of reflection is zero. In other words, if a wave with λ_0 wavelength ($\omega_0 = \frac{2\pi}{\lambda_0}$) have

radiation on a dielectric blade, it has the maximum amount of reflection, if the blade thickness is equal to quarter-wavelength in the material (λ_1).

3- Simulation

3-1- Using multi-layered alternating structures in reflective layers of cells

Today, multi-layered alternating structures have become one of the most important structures in photonic devices. The structures are formed by a series of alternating layers with high and low refractive indices. The alternating changes in refractive indices lead to partial reflection in each two-layer and the sum of these partial reflections causes a reflection of the high gain and proper broadband with arbitrary center by designer. Of the most important alternating multi-layered structures used in this study are: DBR and Chirped DBR.

3-1-1-Using DBR

Some important parameters must be considered in the design of the structure and the first parameter can be the number of two-layers. In other words, taking into account the optimal number of the two-layers, we can obtain a reflection like the

case in which there were many layers. Therefore, increasing the two-layers excessively, the cost of consumables will be increased. According to simulations done, 7 two-layers, compared to other values, is better. Figure 5 shows this clearly. Therefore, this number is considered the design basis and we will use the same number of two-layers in designing. The next step in the design of the DBR structure is selecting the best material for the structure.

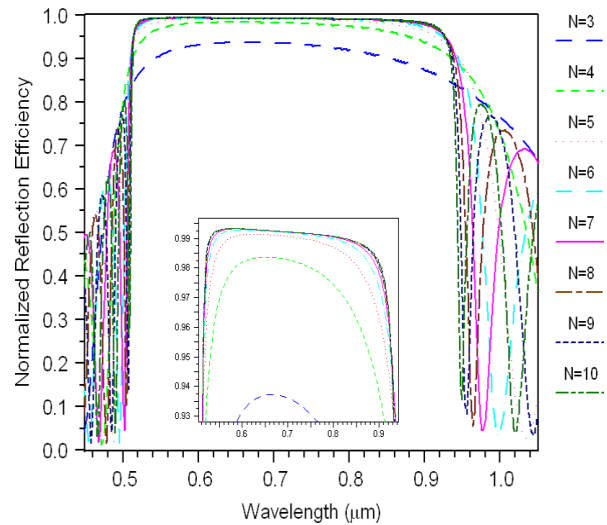


Fig.5. Increase of reflection with the increase of two-layers, where 7 layers is more efficient than others.

Therefore, in the second step we have attempted to select the best material. Figure 6 shows the results. The important point at this stage is that by simulation we achieved the best refractive indices values for two-layers of n_H and n_L , but these values may vary slightly with values in the real world. As a result, we have replaced the obtained optimized values with the nearest refractive indices available in nature.

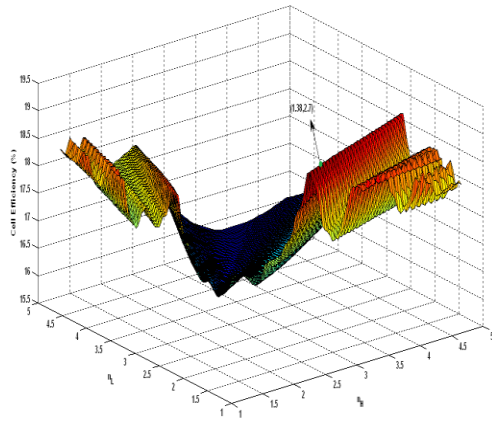


Fig.6. Selecting best material for the desired DBR in solar cell

As is shown in the figure, the best values that can be selected which have the nearest efficiency to the optimized value and their values exist in nature are 2.7 and 1.38 for n_H and n_L . If we want to introduce materials that have these refractive indices, we can present $CuAlSe_2$ for n_H and MgF_2 for n_L . We will use these values and real materials in the later stages of cell simulation. Next, we will examine how much this proposed structure will absorb the of solar radiation spectrum. In other words, we will examine the effects of structure trapping. Solar radiation spectrum in this study is 1.5 AM which is shown in the figure with gray. Figure (7) shows the impact of DBR designed in absorption and trapping of the light in solar cells, compared to the spectrum radiated from the sun. In the following graph we have drawn voltage- cell current, indicating that the current we will receive at the output of the cell will be increased. Figure (8) shows the curve for two different modes. The electrical results of the cell is presented in Table 1. It shows that how much output efficiency and output short circuit current of the cell are optimized.

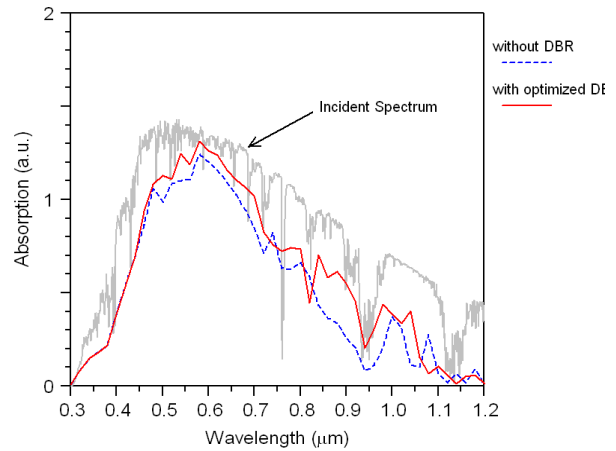


Fig.7. The impact of DBR designed in absorption and trapping of the light in solar cells, compared to the spectrum radiated from the sun.

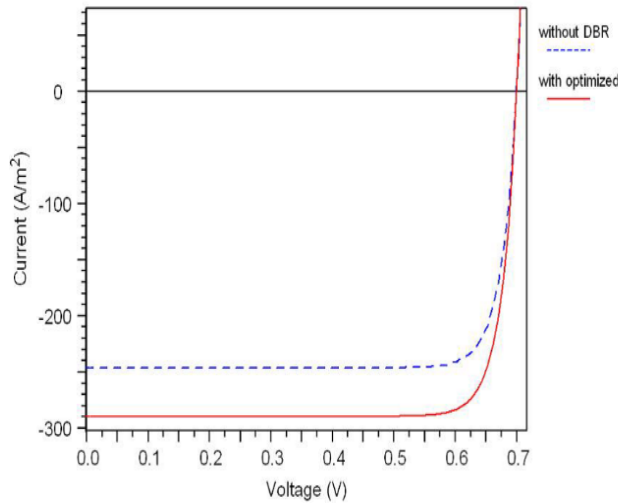


Fig.8. Increase of cell output current due to more light trapping and quantum efficiency increase

Table.1. Results obtained for output efficiency and output short circuit current of the cell

	Solar cell	Total output efficiency in terms of (η) %	output short circuit current of the cell in terms of (J_{sc}) mA/cm ²
1	Without using DBR	16.19	24.62
2	Using optimized DBR	19.04	28.96

3-1-2 Using Chirped DBR

To increase reflection bandwidth and finally increase the returned light to the active area of the cell, we use two DBRs together which forms a Chirped DBR. These two DBRs have two central wavelengths which are a part of the radiation spectrum, and in total, leads to an increase in reflection bandwidth. Thus, in order to design, we consider two samples for λ_{d_1} and λ_{d_2} including 450 and 850 nanometer. We must also note that the number of two-layers should be considered 7 as the previous value. Figure 9 shows the proposed Chirped DBR structure design. The variables that should be calculated are specified in the figure. Structure refractive indices for the first and second DBR are $n \pm \Delta n_1$ and $n \pm \Delta n_2$, respectively. For both DBRs, positive and negative signs indicate a higher refractive index and a lower refractive index, respectively. Then, for both DBRs, we consider higher and lower refractive indices 4.6 and 1.2, respectively. So we have:

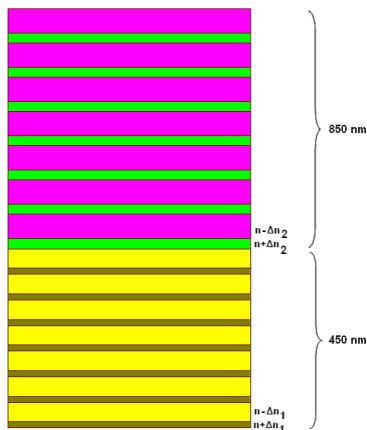


Fig.9.Proposed Chirped DBR structure

$$\text{For 450} \quad \begin{cases} n_{L_1} = n - \Delta n_1 = 1.2 \\ n_{H_1} = n + \Delta n_1 = 4.6 \end{cases} \quad (36)$$

$$\text{For 850} \quad \begin{cases} n_{L_2} = n - \Delta n_2 = 1.2 \\ n_{H_2} = n + \Delta n_2 = 4.6 \end{cases} \quad (37)$$

Now, solving one of the equations of (36) or (37) $n = 2.9$ can be reached. Then, to find the best materials for the layers, we simulate Δn_1 and Δn_2 for the structure in the solar cell, and the obtained results are as follows:

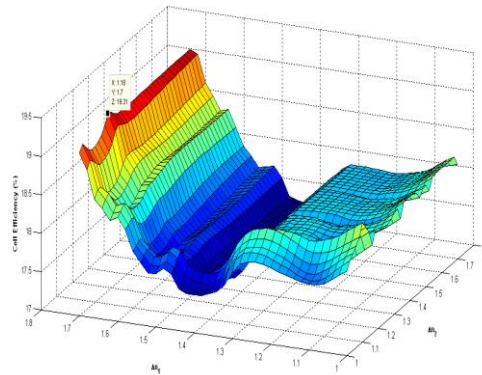


Fig.10.Changes in efficiency in terms of changes in the difference of refraction indices of layers

Ideal amounts are calculated by simulation as $\Delta n_1 = 1.7$ and $\Delta n_2 = 1.18$. Based on these values, the ideal refraction indices for layers are 4.6 and 1.2 for the first DBR 4.08 and 1.72 for second DBR, but we should find the closest actual values in nature for these ideal values; so, doing this we obtain Te (4.6) and MgF2 (1.38) for the first DBR and Ge (4.2) and PbF2 (1.73) for the second DBR. Using this values, we will obtain a result less than the ideal values, because these are actual values and are a bit away from the ideals. Another reason is that since the solar radiation spectrum (Fig. (2-2)) is not

smooth, it cannot be determined precisely, each one reflects which region of the spectrum. To have the maximum reflection by the structure, we should change the values of each DBR central wavelengths in a certain interval to reflect the highest reflection bandwidth and therefore to have the efficiency. Therefore, then we consider the effect of changes in the central wavelength of the DBR on the reflection of total structure and finally the efficiency of solar cells. The obtained results are shown in Fig 11.

As can be seen in Figure (11), optimal values for λ_{d1} and λ_{d2} are 74 nanometer and 731 nanometer, respectively. By applying these values, the efficiency of solar cells is optimized to approximate value of 17.97%. The reason that efficiency of Chirped DBR is higher than DBR is its bandwidth reflection of the structure, which is higher than the one in DBR. It means, compared to the previous mode, this structure reflects a wider bandwidth of the solar spectrum with the same high gain. Plotting the cell voltage-current curve shows that the cell output current is increased. Fig.12. shows the curve for two modes:

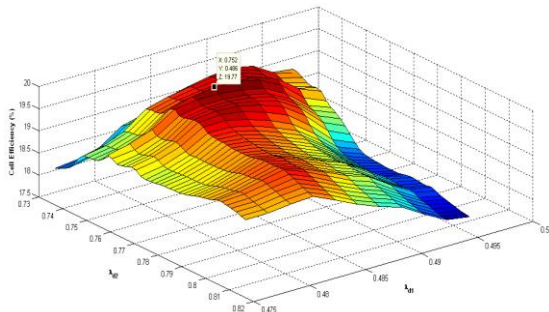


Fig.11.Effect of changes in the central wavelength of the DBR on the efficiency of the solar cell

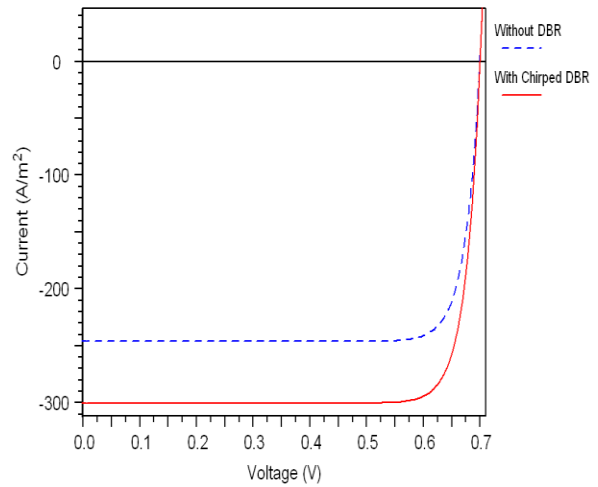


Fig.12.Increase in cell current due to increase in reflection by Chirped DBR

Table.2. Output efficiency and output short circuit current of the cell equipped with Chirped DBR

Solar cell	Total output efficiency in terms of (η) %	output short circuit current of the cell in terms of (J_{sc}) mA/cm ²
Without using DBR	16.19	24.62
Using optimized DBR	19.76	30.05

The cell electrical results, total output efficiency and the cell output short circuit current are presented in Table 2. The Table shows how much they have been optimized

4-Conclusion

Today, due to qualitative growth and scientific advances, energy, especially electricity is increasingly needed by human society. One of the almost endless and pure energy which have been paid attention over the years is the solar energy. Solar cells

directly convert solar energy into electrical energy and are one of the main blocks of photovoltaic systems. Significant improvement has been made in the performance of solar cells since their introduction. Improvement of parameters such as cell efficiency, solar spectrum absorption and manufacturing costs which are key parameters in the process of cell development. The crystalline type is commonly used to achieve a lower recombination and higher absorption coefficient, and other types of silicon that are not used as much have high recombination and low absorption coefficient, leading to a sharp drop in cell efficiency. Different kinds of light trapping techniques and effective photons trapping using some fibered structures and various types of reflecting structures and light scattering, etc., have been proposed. In this paper, distributed Bragg reflector structure and also diffraction grating structure are used. In both structures, determination of the optimum material and also geometric properties to achieve maximum improvement in efficiency have taken into consideration.

References

- [1].M. A. Green, *Solar Cells: Operating Principles, Technology, and System Applications* (Prentice-Hall series in solid state physical electronics). Prentice Hall, 1981, p. 274.
- [2].P. A. Lynn, *Electricity from Sunlight: An Introduction to Photovoltaics*. Wiley, 2010, p. 238.
- [3].“SunShot Vision Study,” no. February, 2012.
- [4].M. a. Green, P. a. Basore, N. Chang, D. Clugston, R. Egan, R. Evans, D. Hogg, S. Jarnason, M. Keevers, P. Lasswell, J. O’Sullivan, U. Schubert, a. Turner, S. R. Wenham, and T. Young, “Crystalline silicon on glass (CSG) thin-film solar cell modules,” *Sol. Energy*, vol. 77, no. 6, pp. 857–863, Dec. 2004.
- [5].R. E. I. Schropp and M. Zeman, *Amorphous and Microcrystalline Silicon Solar Cells: Modeling, Materials and Device Technology*. Kluwer Academic, 1998, p. 207.
- [6].K. Yamamoto, A. Nakajima, M. Yoshimi, T. Sawada, S. Fukuda, T. Suezaki, M. Ichikawa, Y. Koi, M. Goto, T. Meguro, T. Matsuda, M. Kondo, T. Sasaki, and Y. Tawada, “A high efficiency thin film silicon solar cell and module,” *Sol. Energy*, vol. 77, no. 6, pp. 939–949, Dec. 2004.
- [7].J. Müller, B. Rech, J. Springer, and M. Vanecek, “TCO and light trapping in silicon thin film solar cells,” *Sol. Energy*, vol. 77, no. 6, pp. 917–930, Dec. 2004.
- [8].M. Peters, J. C. Goldschmidt, T. Kirchartz, and B. Bläsi, “The photonic light trap—Improved light trapping in solar cells by angularly selective filters,” *Sol. Energy Mater. Sol. Cells*, vol. 93, no. 10, pp. 1721–1727, Oct. 2009.
- [9].S. J. Orfanidis, “Electromagnetic Waves and Antennas,” Rutgers University, 2008. [Online]. Available: <http://eceweb1.rutgers.edu/~orfanidi/ewa/>.
- [10].S. Cloude, *An Introduction to Electromagnetic Wave Propagation & Antennas*. Springer, 1996, p. 200.